IEEE Access
Multidisciplinary | Rapid Review | Open Access Journal

SPECIAL SECTION ON DEEP LEARNING FOR INTERNET OF THINGS

Received July 27, 2021, accepted August 10, 2021, date of publication August 16, 2021, date of current version August 30, 2021.

Digital Object Identifier 10.1109/ACCESS.2021.3105526

Research on Flexible Control Strategy of Controllable Large Industrial Loads Based on Multi-Source Data Fusion of Internet of Things

GUANGYU CHEN[1], XIN ZHANG[1], CHUNHU WANG[2], YANGFEI ZHANG[1], AND SIPENG HAO[1]
[1]School of Electric Power Engineering, Nanjing Institute of Technology, Nanjing 211167, China
[2]State Grid Heilongjiang Electric Power Company, Harbin 150090, China

Corresponding author: Guangyu Chen (cgyhhu@163.com)

This work was supported in part by the Science and Technology Project of Heilongjiang Electric Power Company Ltd., and in part by the Open Fund of the Collaborative Innovation Center of Jiangsu Distribution Network Intelligent Technology and Equipment under Grant XTCX202003.

ABSTRACT With the rapid development of the power grid, the high penetration of new energy sources and the diversity of loads have further aggravated the uncertainty of ''source-load'', which has brought huge challenges to the peak shaving of the power grid. In order to ensure the reliable operation of the power system during the electricity peak, this paper combines the IoT technology to propose a flexible control strategy for controllable large industrial loads that considers the interrupt priority. Firstly, the perception and fusion framework of large industrial load information is constructed based on the IoT technology. After that, the improved TOPSIS method is adopted to establish the evaluation model of the adjustable potentials of large industrial loads and the load interruption priority is further divided. Finally, a three-stage rolling regulation model for controllable large industrial loads to participate in the deep peak shaving of the power grid is constructed to achieve the goal of bidirectional peak shaving on the power generation side and the demand side. The case uses an improved IEEE 30-node system for simulation. As the simulation results show, the method proposed in this paper can not only take the cost of peak load regulation into account, but also effectively achieve the goal of 'peak shaving and valley filling'.

INDEX TERMS Internet of Things, industrial load, interrupt priority, deep peak shaving, rolling regulation.

I. INTRODUCTION

With the high penetration of large-scale new energy, its output volatility and anti-peaking characteristics have seriously affected the adjustment of the power grid peak-valley difference [1]. In addition, the rapid growth of consumer side load has also led to the imbalance of power supply and sales during peak hours. The current peak load regulating of electric power system is facing huge challenges [2].

The traditional peak load regulation of electric power system mainly relies on thermal power units, but with its limited adjustment speed and range, the economy is poor. Furthermore, in recent years, with the high penetration of new energy, their starting capacity is gradually decreasing, and the existing model has had difficulties to adapt to the demand for peak shaving. Therefore, how to coordinate more adjustable resources to participate in power grid peak shaving is a hot issue of current research [3]. Based on the scheduling of cogeneration units, Reference [4] establishes a coordinated regulation model of battery and regenerative electric boiler, which is of great significance to the stable operation of large amounts of wind power infiltration grid. Reference [5] proposes a new power generation control strategy based on the combined regulation of different resources such as large hydroelectric power plants and controllable industrial loads, which greatly improves the power generation efficiency of hydroelectric power plants. Reference [6] proposes an electricity heat hydrogen multi-energy storage system (EHH-MESS) and its coordination and optimization operational model to improve the utilization efficiency of wind power and photovoltaic, avoiding unnecessary abandonment of wind and light. Most above documents

The associate editor coordinating the review of this manuscript and approving it for publication was Yang Xiao.

describe the problems and solutions encountered by new energy in power grid peak shaving from the aspect of energy storage. But they do not thoroughly consider the impact of load-side demand response on the peak shaving of the power grid.

In recent years, as the contradiction between power supply and demand continues to intensify, the difficulty of power grid peak shaving has also increased. Research on the two-way interaction technology between the power generation side and the demand side, represented by the demand side management (DSM) technology, in order to relieve the peak shaving of the power grid, has become a new research hotspot. Reference [7] establishes a bi-level energy-saving dispatching optimization model with the interaction of generation and load on the basis of considering energy-saving and emission-reduction potentials of generation and demand sides, not only considering both the electric power generation cost and the carbon emission cost of thermal units, but also considering both compensation and incentive costs of electricity consumers. Reference [8] establishes an in-day resource trading framework from the point of grid operators (GO), and further establishes the related resource trading model by using the Stackelberg game theory. Reference [9] proposes an optimized economic operation strategy of distributed energy storage with multi-profit mode operation, with a multi-profit model considering three profit modes of distributed energy storage including demand management, peak-valley spread arbitrage and participating in demand response. Reference [10] studies the optimal control model of industrial load under the smart electricity pricing scenarios, and proposes a new industrial load control (ILC) framework, considering the use of renewable energy and energy storage. There are also some scholars who consider this problem more detailed, specific to a certain type of load regulation methods. Reference [11] proposes a cooperative demand response scheme for load management in smart grid, and applies it to the load management of industrial cold storage, which can effectively reduce the electricity costs and curtail the total energy consumption. The above references have conducted research on the issue of demand side involved in power grid peak shaving and achieved good results, but it does not thoroughly consider the specific implementation plan of large industrial loads to participate in peak shaving of the power grid.

Most of the above documents have studied peak shaving methods from the perspective of user demand response, and achieved good adjustment results, but still have the following shortcomings:

(1) There is a lack of research on the load side information panoramic perception, and it fails to root out the potential of different types of large industrial loads involved in demand-side response.

(2) Currently, there are few studies on the regulation of industrial loads (especially large industrial loads), and most studies do not consider the priority of industrial loads regulation, which is less economical and practical.

(3) The existing industrial load dispatching methods are mostly considered from the consumer side and lack holistic thinking (from the perspective of GO). Moreover, the accuracy and stability of control are not high and they are unable to respond to emergency situations that occur in real time.

For existing problems, this paper proposes a flexible control method for large industrial controllable load based on Internet of Things technology. The main contributions of this article are as follows:

(1) It is the first time to build a flexible control architecture for large industrial controllable load based on the IoT technology, using the advantages of the IoT to achieve smoother flexible control of large industrial load.

(2) The paper innovatively establishes a model for large industrial loads adjustable potential evaluation based on the improved TOPSIS evaluation method, and further determines the interrupt priority of large-scale industrial load, applying the priority to formulate a flexible control plan for large industrial controllable load.

(3) In response to the current grid's difficulty in peak shaving, a flexible control strategy for large industrial load considering interrupt priority is proposed and a three-stage (day-ahead, in-day and real-time) rolling control model is established, taking both the goal of 'peak cutting and valley filling' and the economy of system operation into account.

(4) The advantages of the control model of introducing the IoT and load interrupt priority are discussed in detail, which has certain guiding significance for research in related fields and practical engineering applications.

In summary, the specific research work of this paper is as follows:

In the first part, according to the actual application scenarios, we use the IoT technology to build a flexible control architecture for large industrial controllable load to participate in the deep peak shaving of the power grid. In the second part, by consulting the existing references and on-site investigation, we construct an evaluation index system for the adjustable potential of large industrial load and use the improved TOPSIS comprehensive evaluation method to establish an evaluation model, and the K-means clustering analysis algorithm is further used to divide the load interrupt priority. In the third part, considering the stability of the load characteristic curve, with the goal of minimizing the cost of power generation and load regulation, a three-stage rolling control model is constructed. The method proposed in this paper improves the flexible control method of large industrial controllable loads participating in the deep peak shaving of the power grid, and further promotes research on the interactive management of power generation and demand side resources.

Combined with Figure 1, the overall work flow of this article is as follows:

Firstly, this article uses the IoT technology to realize the perception of panoramic information of large industrial loads

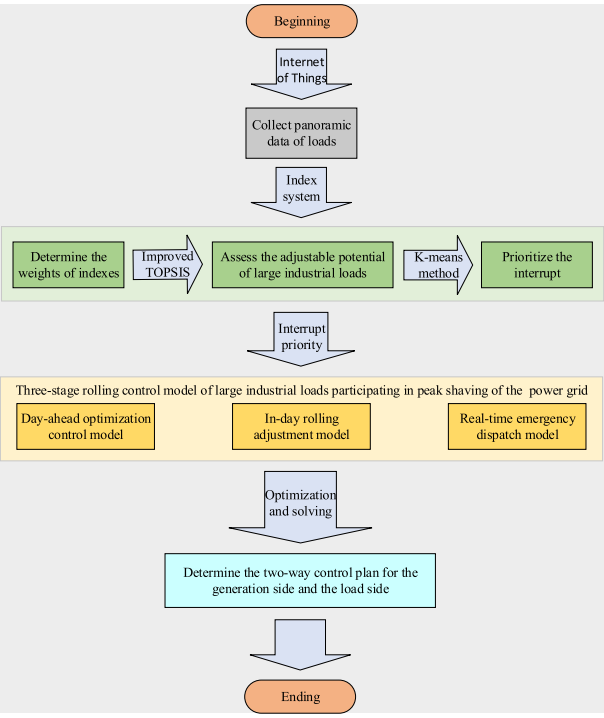

FIGURE 1. The chart of overall work flow.

and provide support for the flexible control of large industrial loads.

Secondly, based on the evaluation index of the adjustable potential of the large industrial load, the comprehensive weighting method is used to determine the weight of each indicator. After that, the improved TOPSIS method is used to establish a comprehensive evaluation model to score the adjustable potentials of large industrial loads. Finally, with the scores as features, the K-means method is used for cluster analysis to divide the interrupt priority of each large industrial load.

Thirdly, through the linear weighted function evaluation method, the three-stage rolling control model (considering the priority of load interruption) of large industrial loads participating in peak shaving of the power grid is optimized and solved, in order to formulate a two-way control plan on the power generation side and the load side.

II. FLEXIBLE CONTROL ARCHITECTURE FOR CONTROLLABLE LARGE INDUSTRIAL LOADS BASED ON INTERNET OF THINGS TECHNOLOGY

A. OVERVIEW OF INTERNET OF THINGS IN POWER SYSTEM

The Internet of Things in Power System (IOTIPS) is a specific application of the IoT [12] in the power industry. It is the information connection and interaction between any time, any place, anyone and anything related to the power industry. As an industrial IoT applied to the power grid, the IOTIPS has the characteristics of comprehensive perception, efficient processing, and flexible applications.

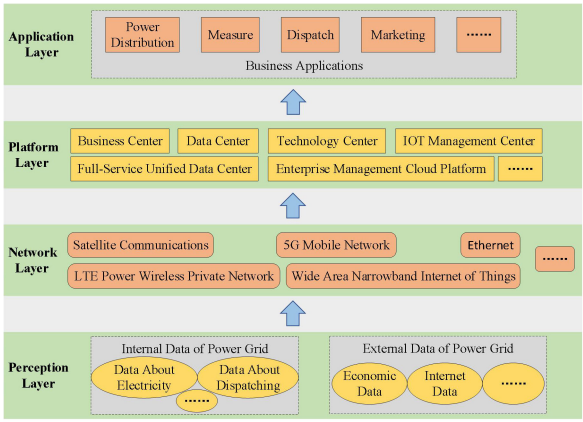

FIGURE 2. The hierarchical architecture of the IOTIPS.

The overall hierarchical structure of the IOTIPS mainly includes four parts: perception layer, network layer, platform layer and application layer, as shown in Figure 2.

At the perception layer, the panoramic and wide-area collection and perception of various information is realized through the unified and standardized access of various terminal data.

At the network layer, information from the perception layer is accessed and transmitted through the existing Internet and other basic network facilities.

At the platform layer, the data transmitted by the network layer can be processed in real time through a unified data center, based on cloud platform algorithms and computing resources.

At the application layer, advanced technologies such as artificial intelligence and big data are used to complete the construction of related advanced applications.

B. MULTI-SOURSE DATA COLLECTION AND FUSION METHOD BASE ON IoT TECHNOLOGY

Considering the aspersion, independence and complexity of the large industrial consumer, this paper applies the IoT technology, which is able to connect massive data entities and realize multi-link data sharing, to realize the collection and integration of large industrial load information.

1) DATA COLLECTION METHOD OF LARGE INDUSTRIAL LOAD

Data collection [13] is the process of collecting sensing data from sensing nodes to sink nodes. It is necessary to ensure the reliable transmission of data and avoid distortion. In the actual data collection process, this paper considers that different large industrial consumers have different interruption characteristics. For example, the continuity of production activities of some large industrial consumers may be relatively low, and the working freedom of each plant in the plant area is relatively high, so that they can separately adjust the electricity load of each plant. While the production activities of other large industrial consumers have high continuity, so that they cannot separately adjust the

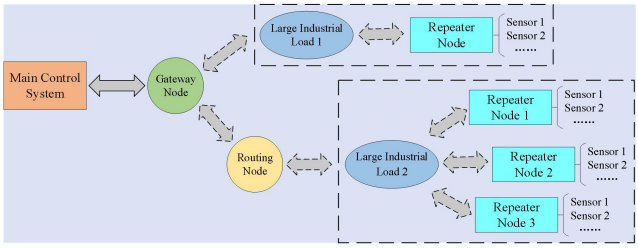

FIGURE 3. The data collection structure diagram of large industrial load.

electricity load of the plants in their plant areas, and they can only adjust the entire plant area as a whole.

For the two different large industrial consumers above, this section uses different data collection methods and sensors for information collection, as shown in Figure 3. For the former (i.e. Load 2 in the figure), in view of the fact that different plants can be controlled separately, the different plants can be used as an independent data collection unit to collect information, and the collected information can be gathered and integrated through the routing node, and then transmitted to the gateway node. For the latter (i.e. Load 1 in the figure), since the object can only achieve overall control, it is taken as a whole unit for data collection, and then transmitted to the gateway node. Finally, after the gateway node receives all the collected data sent to it by other nodes, these data will be summarized and sent to the main control system, and then the main control system will process and save the data.

2) MULTI-DATA SOURCE DATA FUSION PROCESSING STRATEGY

Data fusion technology [14] is a series of theory, technology and methods for processing information from multiple data sources. It is mainly proposed to deal with the problems of data frequency and information overload, by optimizing the multi-source data to reduce data redundancy and improve data processing efficiency.

The panoramic information of large industrial loads that this paper needs to collect also has the characteristics of massive and multiple data sources. It is necessary to introduce data fusion technology to regularly merge and integrate data to provide a reliable guarantee for effective decision-making of managers.

The basic structure of data fusion is generally divided into three layers, according to the degree of fusion, from low to high: data layer, feature layer and decision-making layer. Data layer fusion is the bottommost fusion. Generally, direct calculation is used to extract the required characteristic state quantities from the original data. Feature layer fusion is a medium-level fusion. It usually performs association analysis and feature fusion on the feature quantity in the data source to obtain feature vectors that have a greater effect on state judgment and pattern recognition. As the highest degree of fusion, decision-level fusion generally uses the resulting decision vector to make decisions such as classification, reasoning, identification, and judgment. This paper is mainly

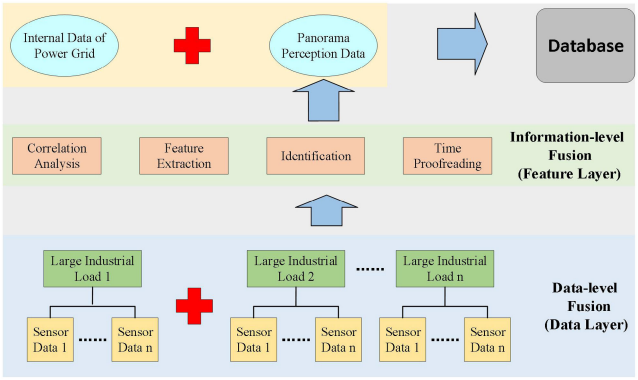

FIGURE 4. The structure diagram of multi-source information fusion of large industrial loads.

to collect panoramic information of large industrial loads, and there is no need to make decisions on the information for the time being.

According to the basic structure of data fusion, combined with the requirements of information sharing, interaction, and high efficiency, this paper builds a three-tier framework for multi-source information fusion of large industrial loads, as shown in Figure 4. In this framework, the data-level fusion is based on the collected raw data, classified and aggregated according to the data category to realize the initial fusion of the collected data. Information-level fusion is to complete the processing of perceptual information through methods such as extraction, correlation, identification and time matching after data-level aggregation, which can fully explain the face of the object. Finally, using data reconstruction, format conversion and other related technologies, the processed data information is deeply integrated with the original internal data in the power grid, and then stored in the database in a unified manner to provide support for the flexible control of large industrial loads.

C. FLEXIBLE CONTROL ARCHITECTURE FOR LARGE INDUSTRIAL CONTROLLABLE LOADS BASED ON IoT INFORMATION

The premise of the application scenario described in this article is: each large industrial consumer is willing to participate in demand response and sign related contracts with power grid companies. The contract stipulates that during the peak period of power load, the power grid company shall, taking the adjustable potential of various industrial loads into account, carry out flexible regulation of these controllable loads to relieve the pressure on the operation of the power grid, and consumers can obtain certain economic compensation. The flexible control architecture of the large industrial controllable load described in this paper is shown in Figure 5, which mainly includes four parts: data source, power generation side, power consumption side and grid dispatching.

With reference to Figure 5, the main process of flexible regulation of large industrial controllable loads which participate in the power grid's deep peak shaving is as follows:

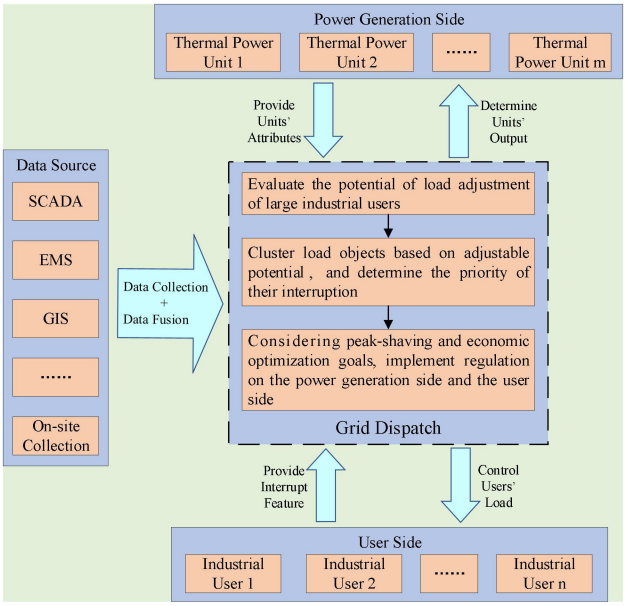

FIGURE 5. The flexible control architecture for large industrial controllable loads based on IoT information.

(1) First, the panoramic information of large industrial loads from different data sources is collected, such as SCADA and GIS, and data fusion processing is performed.

(2) The consumer side reports the load interruption characteristics, such as interruptible time, interruptible capacity. The power generation side provides unit operation attributes, such as start and stop costs, coal consumption costs.

(3) According to the panoramic information of the large industrial load, the load adjustable potential of each industrial consumer is evaluated, and the interrupt priority is divided.

(4) Based on historical operating data of large industrial loads, the load forecasting is proceeded. Considering the goals of the peak-shaving and valley-filling and the economic optimization comprehensively, resources both on the power generation side and the consumer side are regulated.

III. INTERRUPT PRIORITY DIVISION OF CONTROLLABLE LOADS OF LARGE INDUSTRIES

Before implementing flexible regulation on the controllable loads of large industries, this paper needs to evaluate the adjustable potential of various large industrial loads, and divide the interrupt priority of each large industrial load, in order to provide support for the following flexible regulation.

A. COMPREHENSIVE EVALUATION MODEL OF THE ADJUSTABLE POTENTIAL OF LARGE INDUSTRIAL LOADS

1) EVALUATION INDEX SYSTEM OF ADJUSTABLE POTENTIAL OF LARGE INDUSTRIAL LOADS

The load regulation potential of large industrial users refers to the users' demand response capability and the value of users being able to participate in the peak shaving of the power grid. According to the on-site investigations and the research on factors affecting the interrupt characteristics of large industrial loads, this paper selects 16 characteristic indicators from three aspects (characteristics of production and operation, users' electricity characteristics and willingness of load interruption) [15] to construct an index system of adjustable potential evaluation of these loads, as is shown in Figure 6.

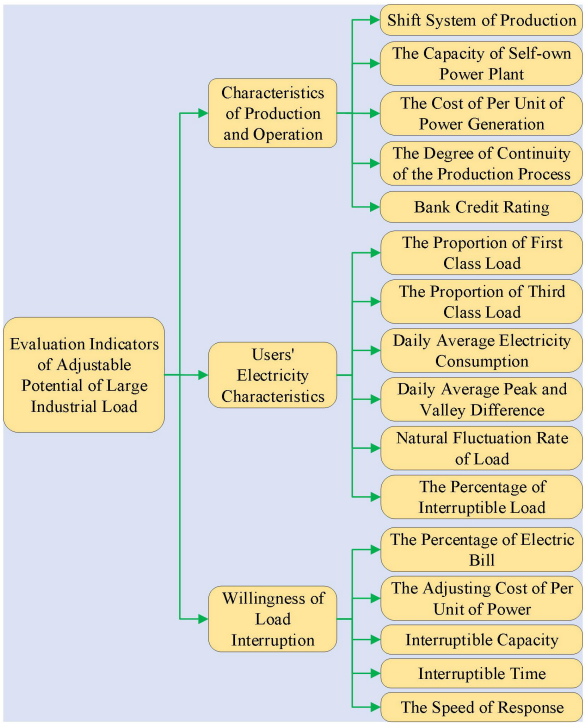

FIGURE 6. An index system for evaluating the adjustable potential of large industrial loads.

2) DETERMINATION OF THE WEIGHTS OF COMPREHENSIVE EVALUATION INDICATORS

The weights of different types of indicators can reflect the amount of information they contain. There are various methods for determining the weights of indicators, but different methods have different focuses. In view of the fact that a single weighting method cannot reflect subjective and objective factors at the same time, this paper combines the G1 method and the CRITIC method to comprehensively consider the impact of subjective factors and objective conditions to obtain composite weight with higher reliability.

The G1 method [16] is also known as the order relation analysis method, which belongs to a commonly used subjective weighting method. The calculation process of this method is simple and fast, and there is no need for consistency verification like the analytic hierarchy process.

The CRITIC method [17] is also called the index importance correlation method, which can be used to deal with the objectively weighting problem under multiple criteria. This method is mainly to determine the objective weight of the indicators by analyzing the objective laws among the indicators.

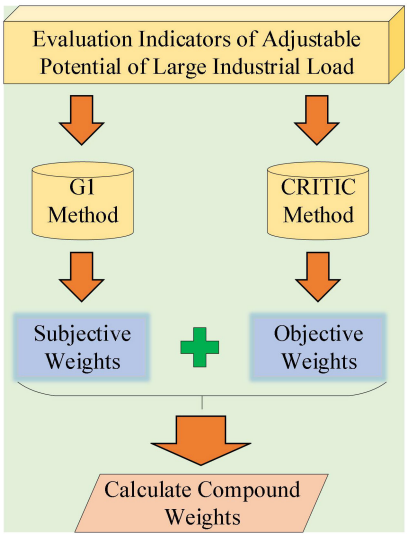

FIGURE 7. The weight determination method of the evaluation index system.

Since it is difficult for a single weighting method to reflect both subjective and objective factors, this section combines the G1 method and the CRITIC method, and comprehensively considers the influence of subjective factors and objective conditions to obtain a highly reliable composite weight.

Figure 7 shows the flow chart of the method for determining the weight of the evaluation index system. The specific steps are as follows:

Step 1. Firstly, the G1 method is used to calculate the subjective weight of each evaluation index.

Step 2. Secondly, the CRITIC method is used to calculate the objective weight of each evaluation index

Step 3. Finally, the final composite weight is calculated by the correction coefficient. The specific calculation method of the composite weight is as follows:

a. Evaluation indicators are arranged in ascending order based on their objective weight.

b. The difference coefficient CY and correction coefficient XZ are calculated.

$$CY = \frac{2}{n} \times \sum_{a=1}^{n} (a \times Cw_a) - \frac{n+1}{n} \tag{1}$$

$$XZ = CY \times \frac{n}{n+1} \tag{2}$$

In the formula, the objective weight vector Cw $(Cw_1, Cw_2, \ldots, Cw_n)$ has been rearranged in ascending order.

c. According to the calculated correction coefficient XZ, the composite weight w of each evaluation index is calculated.

$$w_a = (1 - XZ) \times Gw_a + XZ \times Cw_a \tag{3}$$

In the formula, Gw represents the subjective weights of the evaluation indicators.

3) THE COMPREHENSIVE EVALUATION METHOD OF IMPROVED TOPSIS

The comprehensive evaluation method is an important evaluation method based on the expert evaluation method, which is widely used in the research field of decision analysis. There are many types of comprehensive evaluation methods, such as the analytic hierarchy process, TOPSIS method, grey model method and so on.

The TOPSIS method [18] is also known as technique for order preference by similarity to ideal solution. It is often used in the problem of multi-objective decision-making with limited schemes. Because the traditional TOPSIS method uses Euclidean distance to measure the distance between the different schemes and the positive and negative ideal solutions, there are generally problems of data loss, poor accuracy and poor stability. This article improves the traditional TOPSIS method by using weighting Mahalanobis distance and Tanimoto correlation coefficient to replace Euclidean distance, and comprehensively considers the distance and correlation between the different schemes and the positive and negative ideal solutions to make up for the shortcomings of the traditional method.

Assuming that the set of schemes participating in the evaluation is M $(M_1, M_2, \ldots, M_m)$, and the set of evaluation indicators is D $(D_1, D_2, \ldots, D_n)$, the specific steps of the comprehensive evaluation method of the improved TOPSIS proposed in this paper are as follows:

a. Firstly, the decision matrix X is established, and the value of the evaluation object M_i corresponding to the evaluation index D_j is recorded as y_{ij}.

$$X = \begin{array}{c} \\ M_1 \\ M_2 \\ \vdots \\ M_m \end{array} \begin{array}{c} \begin{array}{cccc} D_1 & D_2 & \cdots & D_n \end{array} \\ \begin{bmatrix} x_{11} & x_{12} & \cdots & x_{1n} \\ x_{21} & x_{22} & \cdots & x_{2n} \\ \vdots & \vdots & \vdots & \vdots \\ x_{m1} & x_{m2} & \cdots & x_{mn} \end{bmatrix} \end{array} \tag{4}$$

b. After that, in accordance with formula (5) and formula (6), dimensionless processing (normalization) is carried out for decision matrix X.

If the value of the index is larger, the higher the regulation potential is, the normalization formula is as follows:

$$x_{ij}^* = \frac{x_{ij} - \min(x_j)}{\max(x_j) - \min(x_j)} \tag{5}$$

If the value of the index is smaller, the higher the regulation potential is, the normalization formula is as follows:

$$x_{ij}^* = \frac{\max(x_j) - x_{ij}}{\max(x_j) - \min(x_j)} \tag{6}$$

Finally, the standardized matrix $X*$ is obtained.

$$X^* = \begin{bmatrix} x_{11}^* & x_{12}^* & \cdots & x_{1n}^* \\ x_{21}^* & x_{22}^* & \cdots & x_{2n}^* \\ \vdots & \vdots & \cdots & \vdots \\ x_{m1}^* & x_{m2}^* & \cdots & x_{mn}^* \end{bmatrix} \tag{7}$$

In the formula, $\min(x_j)$ and $\max(x_j)$ are the minimum and maximum value of the j-th evaluation index respectively.

c. According to the composite weight of the index determined above, the weighted decision matrix R is constructed.

$$R = \begin{bmatrix} r_{11} & r_{12} & \cdots & r_{1n} \\ r_{21} & r_{22} & \cdots & r_{2n} \\ \vdots & \vdots & \cdots & \vdots \\ r_{m1} & r_{m2} & \cdots & r_{mn} \end{bmatrix} \tag{8}$$

Each element r_{ij} in the matrix R is obtained by multiplying the index composite weight W and the dimensionless matrix V. The formula is as follows:

$$r_{ij} = w_j^2 \times w_k^1 \times x_{ij}^* \tag{9}$$

In the formula, w_j^2 and w_k^1 represent the composite weight of the j-th second-level indicator and the composite weight of the corresponding first-level indicator respectively.

d. Then, according to the weighted decision matrix R, the positive and negative ideal solution sample set T^+ and T^- are constructed, and the construction rules are as follows:

$$T_j^+ = \begin{cases} \max(r_j), & D_j \text{ is the bigger, the better.} \\ \min(r_j), & D_j \text{ is the smaller, the better.} \end{cases} \tag{10}$$

$$T_j^- = \begin{cases} \min(r_j), & D_j \text{ is the bigger, the better.} \\ \max(r_j), & D_j \text{ is the smaller, the better.} \end{cases} \tag{11}$$

In the formula, $j = 1, 2, \ldots, n$.

e. According to the weighted decision matrix R, the Tanimoto correlation coefficients (TM^+ and TM^-) between each evaluation object and the positive and negative ideal solutions are calculated to represent the similarity between the decision scheme and the positive and negative ideal solutions.

$$TM_i^+ = \frac{T^+ \cdot r_i}{\left\|T^+\right\|^2 + \|r_i\|^2 - T^+ \cdot r_i} \tag{12}$$

$$TM_i^- = \frac{T^- \cdot r_i}{\left\|T^-\right\|^2 + \|r_i\|^2 - T^- \cdot r_i} \tag{13}$$

In the formula, $||r_{ij}||$ represents the length of the vector composed of all elements in the i-th row of the weighted decision matrix R.

f. The Mahalanobis distances (Md^+ and Md^-) between each evaluation object and the positive and negative ideal solutions are calculated to characterize the difference between them.

$$Md_i^+ = \sqrt{(r_i - T^+)^T \cdot XFC^{-1} \cdot (r_i - T^+)} \tag{14}$$

$$Md_i^- = \sqrt{(r_i - T^-)^T \cdot XFC^{-1} \cdot (r_i - T^-)} \tag{15}$$

In the formula, XFC is the covariance matrix of all samples.

g. According to the calculated Tanimoto correlation coefficient and Mahalanobis distance, the comprehensive state closeness η_i between each evaluation object and the positive ideal solution is calculated. The calculation method is as follows:

$$TJ_i = \frac{TM_i^+}{TM_i^+ + TM_i^-} \tag{16}$$

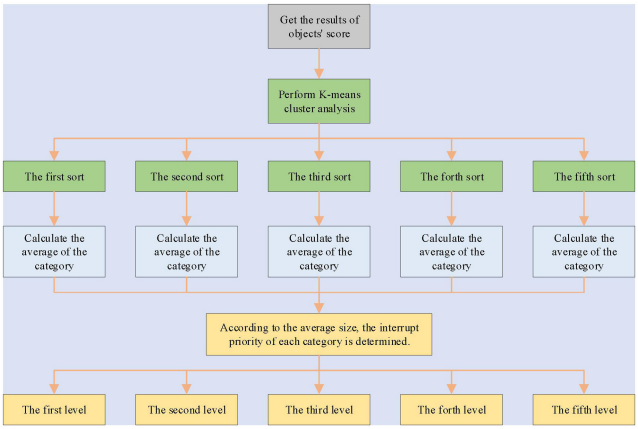

FIGURE 8. The flow chart of the method of dividing the priority of load interruption.

$$MJ_i = \frac{Md_i^-}{Md_i^+ + Md_i^-} \tag{17}$$

$$\eta_i = c \times TJ_i + (1 - c) \times MJ_i \tag{18}$$

The state closeness TJ of the Tanimoto correlation coefficient of each evaluation object is calculated in equation (16). The state closeness MJ of the weighted Mahalanobis distance of each evaluation object is calculated in equation (17). In equation (18), c is the weight coefficient, generally 0.5.

B. THE DIVISION METHOD OF INTERRUPT PRIORITY OF CONTROLLABLE LOAD OF LARGE INDUSTRY

Based on the above evaluation model of adjustable potential of large industrial load, the adjustable potential of industrial users can be quantified as a comprehensive state closeness concisely and clearly. In this section, the adjustable potentials of loads are scored according to their comprehensive state closeness. Then, with the scores as the features, taking the large industrial loads as the objects, the K-means algorithm [19] will be used to cluster analysis, in order to divide their interrupt priority according to their scores.

Figure 8 shows the process of division:

The basic steps are as follows:

a. Firstly, the comprehensive state closeness of each evaluation object is converted into a score under the 100-point system. The formula is as follows:

$$DF_i = 100 \times \eta_i \tag{19}$$

b. The priority of load interruption is divided into 5 levels, that is, the number of clusters is 5.

c. After that, the scores of adjustable potentials and the determined number of clusters are used as input, and the target object is clustered using the K-means algorithm.

d. According to the clustering results, the average scores of all objects in each category are calculated, and recorded as $DF_1, DF_2, DF_3, DF_4, DF_5$.

e. Finally, the average scores of every categories are arranged in descending order. The higher the average score is, the higher the interrupt priority.

TABLE 1. The coefficients of adjusting cost under different interrupt priority levels.

Priority of Load Interruption	Coefficient of Adjusting Cost
0	1.0
1	1.2
2	1.4
3	1.6
4	1.8

Usually, the lower the priority of the load interruption, the higher the cost of adjusting, so we should avoid adjusting these users as much as possible. According to the experience of experts, this paper sets the coefficient of adjusting cost under different interruption priorities in order to support the establishment of the model of large industrial loads participating in the peak shaving of power grid considering interrupt priority, as shown in Table 1.

IV. ROLLING CONTROL STRATEGY OF LARGE INDUSTRIAL CONTROLLABLE LOADS PARTICIPATING IN THE PEAK SHAVING OF POWER GRID

With the aggravation of power supply and demand contradiction, it is difficult to meet the peak shaving requirements of the power system only by adjusting the unit combination on the power generation side during the peak period of power consumption. It is urgent to realize the linkage of demand side resources, and ease the pressure of power grid operation by interrupting part of the industrial load or transferring it to the low power consumption period.

The basic idea of multi-time scales of optimization dispatch of power system is multi-time-level optimization and coordination, and continuous refinement by time-level. On the basis of referring to the traditional rolling dispatching idea, this paper proposes a rolling control strategy based on multi-time scales of large industrial loads participating in the peak shaving of the power grid, as shown in Figure 9.

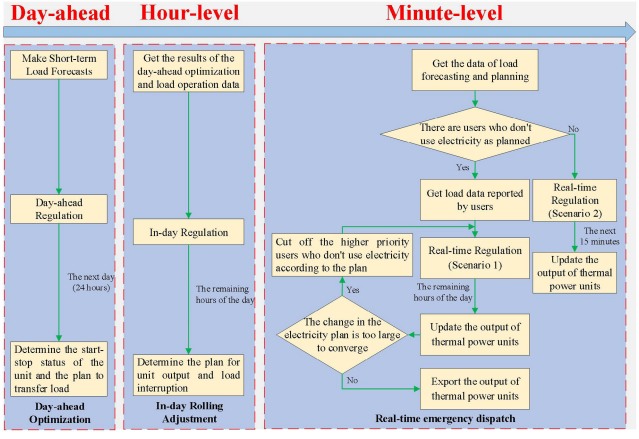

FIGURE 9. The rolling control strategy of large industrial loads participating in the peak shaving of the power grid.

As can be seen from Figure 9, the strategy is mainly divided into three-time scales: day-ahead phase, in-day phase (hour level) and real-time phase (minute level), corresponding to three control links: day-ahead optimization control, in-day rolling adjustment, real-time emergency dispatch.

The scheduling time range of the day-ahead optimization control is 24 hours, and the regulation period is 15 minutes. In this link, it is necessary to forecast the electricity load of the new day based on the recent electricity load data of various industrial users. Then, with this as a benchmark, with the goal of minimizing the cost of thermal power generation and load regulation, taking the effect of 'peak shaving and valley filling' into account, the electricity consumption plan (i.e. transferring power load) in a new day is formulated for industrial users (transferable loads), so as to reduce the load during the peak period and increase the load during the low period, and the start-stop status of the thermal power unit on the power generation side is determined.

The scheduling time range of the in-day rolling adjustment is 4 hours, and the regulation period is 15 minutes. This link is mainly based on the ahead-day plan, and aims at smoothing the load curve and minimizing the cost of regulation. For industrial users (reducible loads), the power consumption plan (i.e. cut off the electricity load) in the remaining period of the day is formulated to reduce the load in the peak period of electricity consumption, and according to the start-stop state of units, the output plan of thermal power units is determined.

The regulation period and scheduling time range of the real-time emergency dispatch are both 15 minutes. This link is mainly to deal with two completely different situations, that is, whether the industrial users participating in peak shaving use electricity according to the established power consumption plan. If all users follow the established power consumption plan, the output of units at the next moment is updated in real time (only for the thermal power units on the generation side) with the single goal of minimizing the cost of power generation. Otherwise, there may be a big difference between the actual power load and the plan. According to the actual circumstances and the start-stop state of units determined previously, the link needs to remake a new output plan for thermal power units during the remaining period of the day with the single goal of minimizing power generation costs. If there are many users who do not use electricity as planned, it results in bigger changes in the power consumption plan, and the units cannot change their output in time to meet the electricity demand. At this time, the electricity load of the users who do not use electricity as planned (with higher priority of interruption) should be forcibly cut off, and the output of units needs to be renewed.

V. ESTABLISHMENT AND SOLUTION OF THE MODEL OF CONTROLLABLE LOADS OF LARGE INDUSTRY THAT PARTICIPATE IN THE DEEP PEAK SHAVING OF THE POWER GRID CONSIDERING INTERRUPTION PRIORITY

In order to ensure the reliable operation of the power system during the peak period of power consumption, this section, based on the economic regulation of resources on the power generation side, combined with the controllable loads of large industry on the demand side to establish the model

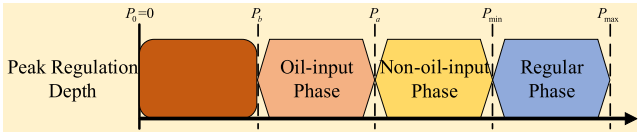

FIGURE 10. The structural diagram of deep peak shaving of the thermal power unit.

of controllable loads of large industry that participate in the deep peak shaving of the power grid considering interruption priority.

In this model, the time of day is divided into 96 parts, and each part is 15 minutes.

A. THE MODEL OF CONTROLLABLE LOADS OF LARGE INDUSTRY AND THERMAL POWER UNITS

1) PEAK-SHAVING COST OF THERMAL POWER UNITS

According to the combustion state and energy consumption characteristics, the peak-shaving process of thermal power units can be divided into three stages: regular phase, oil-input phase and non-oil-input phase [20]. As is shown in Figure 10, when the output of the thermal power unit is between the maximum value P_{max} and the minimum value P_{min}, the unit operates in the regular phase. When the thermal power unit reduces its output to between P_{min} and P_a (minimum output of stable combustion without fuel injection during deep peak shaving), the unit operates in the oil-input phase. When the output of the thermal power unit is further reduced buy fuel injection to support combustion, so that the output is between P_a and P_b (minimum output of stable combustion with fuel injection during deep peak shaving), the unit operates in the non-oil-input phase.

The peak-shaving cost of the thermal power unit is mainly composed of the cost of coal consumption, the cost of loss of unit's life, the cost of fuel consumption in the oil-input phase and the cost of environmental penalty.

a: THE COST OF COAL CONSUMPTION

In different peak-shaving stages, the coal consumption cost of thermal power units is different, which can be fitted as different functions.

$$C_{coal} = \begin{cases} a_i \times q_{ij}^2 + b_i \times q_{ij} + c_i, & P_{\min} < q_{ij} < P_{\max} \\ g_i \times q_{ij} + h_i, & P_b < q_{ij} < P_{\min} \end{cases} \tag{20}$$

In the formula, q_{ij} represents the output of the thermal power unit, a_i, b_i, and c_i are the coefficients of the coal consumption cost of the thermal power unit under the regular phase, and g_i and h_i are the coefficients of the coal consumption cost of the thermal power unit under other deep peak-shaving phases.

b: THE COST OF LOSS OF UNIT'S LIFE

In the non-oil-input phase, the service life of the thermal power unit will be reduced due to the alternating stress. This paper refers to the Manson-Coffin formula [21] to calculate the loss cost of the unit.

$$C_{unit\_loss} = \frac{\lambda \times S_{unit}}{2 \times N_f(q_{ij})} \tag{21}$$

$$N_f(q_{ij}) = 0.00577 \times q_{ij}^3 + 2.682 \times q_{ij}^2 + 484.8 \times q_{ij} - 8411 \tag{22}$$

In the formula, λ is the loss coefficient of the thermal power unit, S_{unit} is the purchase cost of the thermal power unit, and $N_f(q_{ij})$ represents the number of rotor cracking cycles.

c: THE COST OF FUEL CONSUMPTION IN THE OIL-INPUT PHASE

In the oil-input phase, the thermal power unit needs to inject oil to support combustion in order to maintain the stable operation of the boiler combustion. The fuel consumption cost incurred at this time is:

$$C_{oiling} = S_{oil} \times Q_{oil} \tag{23}$$

$$Q_{oil} = \beta \times T_{oil} \tag{24}$$

In the formula, Q_{oil} represents the fuel consumption required. S_{oil} represents the oil price. β represents the fuel consumption rate of the unit. T_{oil} represents the time for the oil-input phase.

d: THE COST OF ENVIRONMENTAL PENALTY

In view of the emission characteristics of the thermal power unit, this paper refers to the previous references [22] and [23], taking the environmental benefits of the unit into consideration. And it is fitted to the form of quadratic function as follows:

$$C_{pollute,1} = \mu \times (A_i \times q_{ij}^2 + B_i \times q_{ij} + C_i) \tag{25}$$

In the formula, μ is the penalty coefficient of environmental pollution, and A_i, B_i, and C_i are the emission coefficients of thermal power units respectively.

In addition, after the unit is fueled and burned, a large number of additional pollutants will be generated during the oil-input phase, which will increase the emission costs. The calculation formula for this part is as follows:

$$C_{pollute,2} = \alpha \times Q_{oil} \tag{26}$$

In the formula, α is the cost coefficient of pollutant discharge treatment.

Combining equation (25) and equation (26), the environmental penalty cost can be expressed as:

$$C_{pollute} = \begin{cases} C_{pollute,1}, & P_a < q_{ij} < P_{\max} \\ C_{pollute,1} + C_{pollute,2}, & P_b < q_{ij} < P_a \end{cases} \tag{27}$$

In summary, the peak-shaving cost of the thermal power unit can be represented by the following piecewise function.

$$C_{fire} = \begin{cases} C_{pollute} + C_{coal}, \\ \quad P_{\min} < q_{ij} < P_{\max} \\ C_{pollute} + C_{coal} + C_{unit\_loss}, \\ \quad P_a < q_{ij} < P_{\min} \\ C_{pollute} + C_{coal} + C_{unit\_loss} + C_{oiling}, \\ \quad P_b < q_{ij} < P_a \end{cases} \tag{28}$$

2) INDUSTRIAL LOAD BELONGING TO REDUCIBLE LOAD

The industrial load belonging to reducible load [24] refers to the industrial user object that can directly cut off all or part of its electricity load during the peak period of electricity consumption.

Set 0-1 variable R_i^{cut} to indicate whether to reduce the power load of the industrial user. And when R_i^{cut} is equal to 1, it means to reduce the power load of the user.

If an industrial load belongs to reducible load, the following content needing to be specified in the contract includes fixed compensation fee e_i^{fixcut} for load reduction, compensation price e_i^{cut} for reducing load per unit power, the start time $T_{i.cut}^{start}$ and end time $T_{i.cut}^{over}$ that the load can be reduced and capacity P_i^{cut} of load that can be reduced.

After the reducible load is regulated, the power load of the industrial user changes as follows:

$$p'_{ij} = p'_{ij} - P_i^{cut}, \quad T_{i.cut}^{start} \le j < T_{i.cut}^{over} \tag{29}$$

In the formula, p'_{ij} represents the power load of the user at the j-th moment.

The compensation costs arising from the regulation are as follows:

$$C_{reduce}^{i} = R_i^{cut} \times (e_i^{fixcut} + e_i^{cut} \times \sum_{j=T_{i.cut}^{start}}^{T_{i.cut}^{over}-1} P_i^{cut}) \tag{30}$$

In addition, the reduction of users' electricity load will inevitably lead to the loss of electricity revenue. The calculation formula is as follows:

$$C_{reduce\_bill}^{i} = R_i^{cut} \times \sum_{j=T_{i.cut}^{start}}^{T_{i.cut}^{over}-1} d_j \times P_i^{cut}/4 \tag{31}$$

In the formula, d_j represents the time-of-use electricity price.

3) INDUSTRIAL LOAD BELONGING TO TRANSFERABLE LOAD

Compared with the reducible load, the industrial load belonging to transferable load [25] has the continuity of electricity consumption. If it is directly interrupted, it will often cause greater economic losses. Therefore, for this type of load, it can only be transferred as a whole. The electricity load during the peak period of power consumption is transferred to the trough period.

Set the 0-1 variable R_i^{shift} to indicate whether to transfer the power load of the industrial user, and when R_i^{shift} is equal to 1, it means transferring the power load of the user.

If an industrial load belongs to a transferable load, the following content needs to be specified in the contract includes the compensation price coefficient e_i^{shift} for transferring load per unit power, the start time $T_{i.shift}^{start}$ and end time $T_{i.shift}^{over}$ that the load can be transferred and the beginning and end time period $(t_{i.down}^{shift}, t_{i.up}^{shift})$ of the acceptable transfer period.

After the transferable load is regulated, the power load of the industrial user changes as follows:

$$p'_{i[t_i^{s.shift}, t_i^{s.shift}+T_{i.shift}^{over}-T_{i.shift}^{start}-1]} \leftrightarrow p'_{i[T_{i.shift}^{start}, T_{i.shift}^{over}-1]} \tag{32}$$

In the formula, $\leftrightarrow$ represents the exchange of element values.

The compensation costs arising from the regulation are as follows:

$$C_{shift}^{i} = R_i^{shift} \times e_i^{shift} \times \left| T_{i.shift}^{start} - t_i^{s.shift} \right| \times \sum_{j=T_{i.shift}^{start}}^{T_{i.shift}^{over}-1} p'_{ij} \tag{33}$$

In the formula, $t_i^{s.shift}$ represents the starting time after the load is transferred. The compensation price $e_i^{shift} \times \left| T_{i.shift}^{start} - t_i^{s.shift} \right|$ that represents the compensation price coefficient for transferring load per unit power can be described as an inverted triangle curve. The larger the distance between the time period after transfer and the original, the higher the compensation price required, as shown in Figure 11.

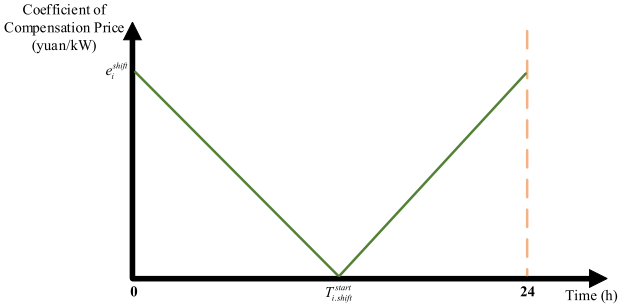

FIGURE 11. The compensation price coefficient curve for transferring load per unit power.

Similarly, after the user's load is transferred, it will also cause the loss of electricity revenue. The calculation formula is as follows:

$$C_{shift\_bill}^{i} = \sum_{j=1}^{96} d_j \times \left(p'_{ij} - p_{ij} \right) /4 \tag{34}$$

In the formula, p_{ij} is the changed electricity load after regulation.

In addition, the conditions that the transferable load needs to meet include:

(1) The constraints of the transferable time of the load:

$$t_{i.down}^{shift} \le t_i^{s.shift} \le t_{i.up}^{shift} - T_{i.shift}^{over} + T_{i.shift}^{start} \tag{35}$$

$$(t_{i.down}^{shift}, t_{i.up}^{shift}) \cap (T_{i.shift}^{start}, T_{i.shift}^{over}) = \emptyset \tag{36}$$

(2) The constraint that total amount of electricity load remains constant:

$$\sum_{j=1}^{96} p_{ij} = \sum_{j=1}^{96} p'_{ij} \tag{37}$$

(3) The constraint on response time of the load objects:

$$t_i^{s.shift} - T \geq 4 \times s_i \tag{38}$$

In the formula, T represents the current moment of implementing regulation, and s_i represents the response time required by the user from receiving the electricity plan to executing it.

B. THE DAY-AHEAD REGULATION MODEL BASED ON JOINT PEAK SHAVING

Considering that the time span required to adjust the transferable type of industrial load is generally large, the regulation process of this type of load is given priority in the day-ahead optimization model.

There are two goals in the day-ahead optimization model. One is to minimize the cost of thermal power generation and load regulation, and the other is to ensure the peak load reduction effect in the peak load period as far as possible. According to the forecasted electricity load in the new day, the model can be solved to obtain the following variables: the start-stop state matrix Z of the thermal power unit, the electricity transfer plan of industrial users (that are, the variables R_i^{shift} and $t_i^{s.shift}$), and they are regarded as known quantities, brought into the in-day and real-time optimization decision.

The specific objective functions of the model are:

$$\begin{cases} F_1 = \min(f_{c1}, f_{p1}) \\ f_{c1} = \sum_{i=1}^{m2} (C^i_{shift\_bill} + y_i \times C^i_{shift}) \\ + \sum_{i=1}^{u1+u2+u3} \sum_{j=1}^{96} z_{ij} \times C_{fire} \\ + \sum_{i=1}^{u1+u2+u3} \sum_{j=2}^{96} \left[\begin{array}{l} w_i^s \times round\left(\frac{2z_{ij}-2z_{i(j-1)}+1}{4}\right) \\ + w_i^o \times round\left(\frac{2z_{i(j-1)}-2z_{ij}+1}{4}\right) \end{array} \right] \\ f_{p1} = \sum_{j=1}^{96} \left| \sum_{i=1}^{u1+u2+u3} q_{ij} - \sum_{i=1}^{m1+m2} p_{ij} - TP_j \right| \end{cases} \tag{39}$$

In the formula, $m1$ and $m2$ represent the total number of industrial loads belonging to transferable and reducible load, $u1$, $u2$ and $u3$ represent the number of thermal power units operating in the regular, non-oil-input and oil-input phase, y_i is the adjusting cost coefficients corresponding to users with different interruption priorities in Table 1, TP_j represents the forecasting data of the load without adjustable loads at 96 points in a day, w_i^s and w_i^o represent the start-up and shut-down cost of the thermal power unit, z_{ij} represents the start-stop state of the i-th thermal power unit at the j-th moment (set 1 in the start-up state, and 0 in the shut-down state), The function $round()$ represents rounding.

The constraints of the model are:

(1) The power constraint of system:

In order to ensure that each user can get sufficient power supply, the total output of the generator set at a certain time needs to be greater than or equal to the total power load.

$$\sum_{i=1}^{u1+u2+u3} q_{ij} \geq \sum_{i=1}^{m1+m2} (p_{ij} + TP_j) \tag{40}$$

In the formula, j does not include the peak period.

(2) The output constraints of the thermal power unit:

The upper and lower limits of the output of thermal power units are:

For the unit operating in the regular phase,

$$z_{ij} \times q_{i.\min} \leq q_{ij} \leq z_{ij} \times q_{i.\max} \tag{41}$$

For the unit operating in the non-oil-input phase,

$$z_{ij} \times q_{i.a} \leq q_{ij} \leq z_{ij} \times q_{i.\min} \tag{42}$$

For the unit operating in the oil-input phase,

$$z_{ij} \times q_{i.b} \leq q_{ij} \leq z_{ij} \times q_{i.a} \tag{43}$$

In the formula, $q_{i.min}$ and $q_{i.max}$ represent the minimum and maximum output of the thermal power unit, $q_{i.a}$ represents the minimum output of stable combustion without fuel injection during deep peak shaving, and $q_{i.b}$ represents the minimum output of stable combustion with fuel injection during deep peak shaving.

The climbing constraint of the thermal power unit are:

$$-r_{i.down} \leq q_{ij} - q_{i(j-1)} \leq r_{i.up} \tag{44}$$

In the formula, $r_{i.down}$ and $r_{i.up}$ are the maximum downward and upward climbing rate of the thermal power unit.

(3) The start and stop constraints of the thermal power unit:

The constraints of the minimum start-stop time of thermal power units are:

$$\sum_{j=0}^{4\times T_{i.on}-1} z_{i(j+t)} \geq 4 \times T_{i.on} \times \left| z_{i(j+t)} - z_{i(j+t-1)} \right| \tag{45}$$

$$\sum_{j=0}^{4\times T_{i.off}-1} \left(1 - z_{i(j+t)}\right) \geq 4 \times T_{i.off} \times \left| z_{i(j+t)} - z_{i(j+t-1)} \right| \tag{46}$$

In the formula, $T_{i.on}$ and $T_{i.off}$ indicate the minimum continuous start-up and shut-down time of the unit.

(4) The constraints of spinning reserve:

In order to deal with emergencies, the thermal power units need to reserve a certain amount of positive and negative spinning reserve to ensure the safe operation of the power grid.

$$\sum_{i=1}^{u1+u2+u3} z_{ij} \times \left(q_{i.\max} - q_{ij}\right) \geq X_{up} \tag{47}$$

$$\sum_{i=1}^{u1+u2+u3} z_{ij} \times \left(q_{ij} - q_{i.\min}\right) \geq X_{down} \tag{48}$$

In the formula, X_{up} and X_{down} represent the capacity of positive and negative spinning reserve.

C. THE IN-DAY ROLLING CONTROL MODEL BASED ON JOINT PEAK SHAVING

On the basis of the ahead-day optimization results, the in-day rolling adjustment model rolls every 4 hours, aiming at the relative smoothness of the load curve and the minimization of the regulation cost of resources on generation side and demand side. The following variables solved and obtained include the output matrix Q of thermal power units, the power interruption plan of industrial users (i.e. the variable R_i^{cut}), and they are regarded as known quantities, brought into the real-time optimization decision.

The specific objective functions of the model are as (49), shown at the bottom of the page.

In the formula, $k \in \{0,1,2,3,4,5\}$ indicates that the current rolling number is $k+1$, and $km1$ indicates the total number of load objects available for reduction during this rolling.

The constraints of the model are:

(1) The number constraints of rolling control:

There are 24 hours in a day, and the cycle is once every 4 hours, so the maximum number of scrolling is 6 times.

$$0 \leq k \leq 5 \quad \text{and } k \in Z \tag{50}$$

(2) The power constraint of system:

$$\sum_{i=1}^{u1+u2+u3} q_{ij} \geq \sum_{i=1}^{m1+m2} (p_{ij} + TP_j) \tag{51}$$

(3) The output constraints of the thermal power unit:

It is the same as the constraints of day-ahead dispatching and will not be repeated here.

(4) The constraints of spinning reserve:

It is the same as the constraints of day-ahead dispatching and will not be repeated here.

D. THE REAL-TIME EMERGENCY CONTROL MODEL BASED ON JOINT PEAK SHAVING

After the optimization decision of the day-ahead and in-day control link, the regulation of demand-side resources has been completed. The real-time emergency dispatch is mainly to slightly adjust the output of thermal power units under the condition that the power load is determined, with the single goal of the minimization of the power generation cost.

There are two main scenarios in the real-time emergency dispatch model. One is that the industrial users can not execute the power consumption plan, so that the electricity load may change greatly at this time. The output of the units in all remaining time periods can be obtained by solving the model to ensure sufficient power supply. The other is that all industrial users follow the established power consumption plan. At this time, the model is solved to obtain the output of the unit at the next moment, which is updated in real time.

1) SCENE 1

The objective function of the model under the scene 1 is:

$$F_{31} = \min\left(\sum_{i=1}^{u1+u2+u3} \sum_{j=l+1}^{96} z_{ij} \times C_{fire}\right) \tag{52}$$

In the formula, l represents the current time for the real-time scheduling.

At this time, the constraints are:

(1) The constraints of regulation time:

$$1 \leq l \leq 95 \text{ and } l \in Z \tag{53}$$

(2) The power constraint of system:

It is the same as the constraints of in-day dispatching and will not be repeated here.

(3) The output constraints of the thermal power unit:

It is the same as the constraints of day-ahead dispatching and will not be repeated here.

(4) The constraints of spinning reserve:

It is the same as the constraints of day-ahead dispatching and will not be repeated here.

2) SCENE 2

The objective function of the model in the scene 2 is:

$$F_{32} = \min\Bigg(\sum_{i=1}^{u1+u2+u3} z_{ij} \times C_{fire}\Big|_{j=l+1} + \sum_{i=1}^{u1+u2+u3} \left[G_i \times \left|q_{i(l+1)} - q'_{i(l+1)}\right| + H_i\right]\Bigg) \tag{54}$$

$$\begin{cases} F_2 = \min(f_{c2}, f_{p2}) \\ f_{c2} = \sum_{i=1}^{km1} \left(C^i_{reduce\_bill} + y_i \times C^i_{reduce}\right) + \sum_{i=1}^{u1+u2+u3} \sum_{j=16\times k+1}^{96} z_{ij} \times C_{fire} \\ f_{p2} = \sqrt{\sum_{j=16\times k+1}^{96} \frac{[(\sum_{i=1}^{m1+m2} p_{ij} + TP_j) - \sum_{j=16\times k+1}^{96} (\sum_{i=1}^{m1+m2} p_{ij} + TP_j)/(96 - 16 \times k)]^2}{(96 - 16 \times k)}} \end{cases} \tag{49}$$

TABLE 2. The data of transferable load in the contract.

User Object	Load 1	Load 2	Load 3	Load 4
Compensation Price Coefficient for Transferring Load Per Unit Power (yuan/kW)	0.31	0.61	0.43	0.20
The Start Time that the Load can be Transferred	31	26	41	34
The End Time that the Load can be Transferred	50	45	60	64
The Beginning of the Acceptable Transfer Period	1	75	1	65
The End of the Acceptable Transfer Period	30	96	40	96

In the formula, $q'_{i(l+1)}$ represents the in-day output plan of thermal power units, $q_{i(l+1)}$ represents the output of thermal power units after real-time adjustment, and G_i and H_i are the adjusted output cost coefficients of the thermal power unit.

The constraints of the model are the same as those in scene 1, so it will not be repeated.

E. THE SELECTION OF COMPROMISE SOLUTIONS FOR MULTI-OBJECTIVE OPTIMIZATION

For the day-ahead and in-day multi-objective model established above, this paper adopts a multi-objective optimization method (linear weighted evaluation function method) to reconstruct the multi-objective function $F = \min(f_c, f_p)$ into the single objective function $\min(F')$. Then, the model is optimized and solved.

$$F' = K_1 \times f_c + K_2 \times f_p \tag{55}$$

In the formula, K_1 and K_2 are weighted coefficients, which can be calculated by the following method.

$$K_1 = \frac{f_p^1 - f_p^2}{(f_c^2 - f_c^1) + (f_p^1 - f_p^2)} \tag{56}$$

$$K_2 = \frac{f_c^2 - f_c^1}{(f_c^2 - f_c^1) + (f_p^1 - f_p^2)} \tag{57}$$

In the formula, f_c^1 and f_p^2 represent the minimum value of the objective function f_c and f_p, f_c^2 / f_p^1 represents the function value of f_c / f_p when the objective function f_p / f_c obtains the minimum value.

VI. CASE ANALYSIS

A. CASE PARAMETERS

This article uses an improved IEEE 30-node system for analysis, which is shown in Figure 20 in the appendix. Assuming that there are 8 large industrial users in the system willing to participate in the peak regulation of the power grid, where Load 1 corresponds to Node 4, Load 2 corresponds to Node 10, Load 3 corresponds to Node 12, Load 4 corresponds to Node 15, Load 5 corresponds to Node 6, Load 6 corresponds to Node 24, Load 7 corresponds to Node 28, and Load 8 corresponds to Node 25. Among them, Load 1 and Load 3, Load 5 and Load 7 are respectively different plant areas of the same large industrial user, which can be controlled separately through the use of the Internet of Things technology.

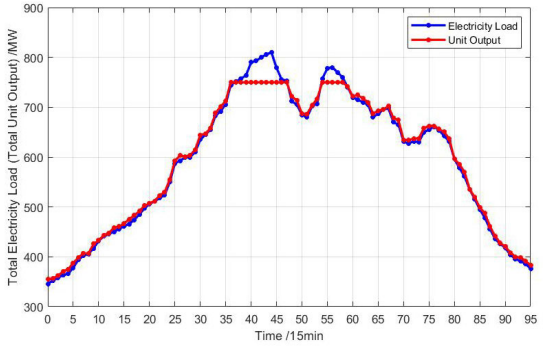

FIGURE 12. The data of electricity load and unit output.

1) CONTROLLABLE LARGE INDUSTRIAL LOAD

Load 1, Load 2, Load 3 and Load 4 belong to transferable loads, and data of their interactive contract with power grid companies are shown in Table 2. Load 5, Load 6, Load 7, Load 8 belong to reducible loads, and data of their interactive contract with the grid company are shown in Table 3.

2) THERMAL POWER UNITS

In this application scenario, the operating loss coefficient of thermal power units λ are respectively 1.2 and 1.5 during oil-input and non-oil-input phase. The oil consumption rate of the units during oil-input phase is 4.8 t/h and the current oil price is 6200 yuan/t. In addition, the environmental pollution punishment coefficient of each thermal power unit is 5000 yuan/t, and the cost coefficient of pollutant discharge treatment is 25 yuan/t.

3) PEAK-VALLEY ELECTRICITY PRICE AND LOAD DATA

In this example, we refer to the actual peak-valley electricity price of a province, and set the electricity price parameters as shown in Table 4.

In this paper, the electricity load and unit output value of the improved IEEE 30-node system in a day are shown in Figure 12.

In Figure 12, the blue and red lines represent the total electricity load of the user and the total output of the unit within a day. It can be seen that in this system, electricity load has two peak periods [35], [45] and [54], [58]. At this time, the unit has been fully loaded, and it is necessary to properly regulate load resources on the demand side to meet the requirements of stable operation of the power system.

TABLE 3. The data of reducible load in the contract.

User Object	Load 5	Load 6	Load 7	Load 8
Fixed Compensation Fee for Load Reduction (yuan)	6.28	6.47	6.47	5.52
Compensation Price for Reducing Load Per Unit Power (yuan/kW)	1.99	1.89	1.02	1.26
The Start Time that the Load can be Reduced	50	37	55	25
The End Time that the Load can be Reduced	70	48	76	48
Capacity of Load that can be Reduced (MW)	20	30	14	10

TABLE 4. The peak-valley electricity price parameters.

Electricity Price	Price (yuan/kWh)	Time Period
Peak Period	3.11	8:00—20:00
Normal Period	2.42	7:00—8:00 20:00—23:00
Valley Period	1.34	0:00—7:00 23:00—24:00

TABLE 5. The weight values for first-level indicators.

First-level Indicators' Name	Weight Coefficient
Characteristics of Production and Operation	0.30
Users' Electricity Characteristics	0.25
Willingness of Load Interruption	0.45

B. ANALYSIS OF RESULTS

1) ANALYSIS OF THE RESULTS OF INTERRUPT PRIORITY DIVISION

First of all, consulting the opinions of many experts, using G1 method to determine the weights of first-level indicators, the results are shown in Table 5.

Then the weights of the second-level indicators are determined by the method for calculating comprehensive weights proposed in section 2. The results are shown in Table 6.

a: EVALUATION RESULTS OF THE IMPROVED TOPSIS METHOD

After the weights of each index determined, the improved TOPSIS method proposed in this paper is used to evaluate the adjustable potentials of the eight large industrial users. The specific scoring results are shown in Table 7.

Finally, the K-means clustering algorithm is used to cluster the scoring results, and the interrupt priority of each large industrial load is divided, as shown in Table 8.

In order to show the clustering results more intuitively, this case uses the histogram to show the interrupt prioritization results listed in Table 8, as shown in Figure 13.

It can be seen from Figure 13 that there are three industrial users in the first echelon of interrupt priority of loads, two in the third echelon and one in each of the remaining echelons.

b: THE COMPARATIVE ANALYSIS BETWEEN THE TRADITIONAL TOPSIS METHOD AND THE IMPROVED TOPSIS METHOD

Using the comprehensive evaluation method of the traditional TOPSIS, the specific scoring results are shown in Table 9.

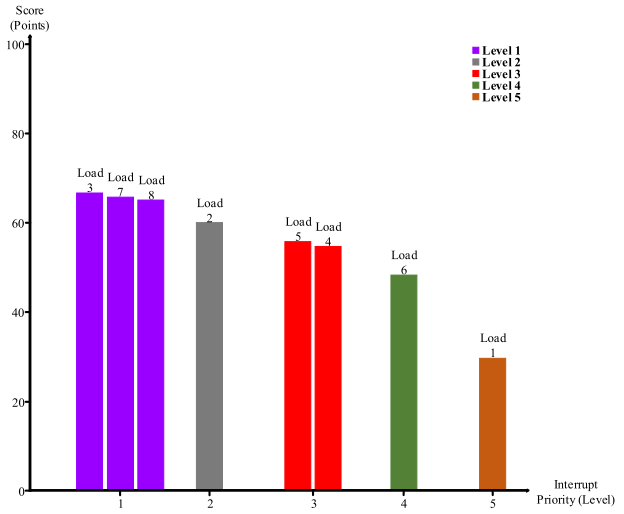

FIGURE 13. The clustering results of adjustable potential of large industrial loads.

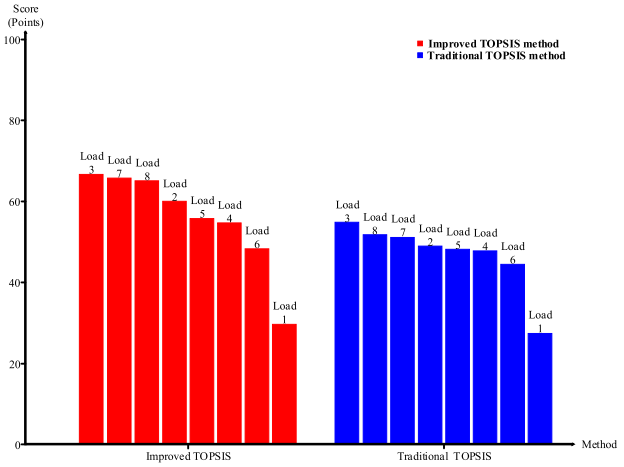

FIGURE 14. The comparison between results of the improved TOPSIS method and the traditional TOPSIS method.

The scoring results obtained from the traditional TOPSIS method are compared with those from the improved TOPSIS method and presented in the form of histogram, as shown in Figure 14.

As can be seen from Figure 14, compared with the traditional TOPSIS method, the improved TOPSIS method has a wider numerical span, stronger discrimination and better evaluation effect.

2) ANALYSIS OF THE RESULTS OF THE REGULATION MODEL

According to the interruption priority of large industrial consumers, the regulation plan of resources on the power

TABLE 6. The weight values for second-level indicators.

First-level Indicators' Name	Second-level Indicators' Name	Weight Coefficient
Characteristics of Production and Operation	Shift System of Production	0.29
	The Capacity of Self-own Power Plant	0.16
	The Cost of Per Unit of Power Generation	0.15
	The Degree of Continuity of the Production Process	0.26
	Bank Credit Rating	0.14
Users' Electricity Characteristics	The Proportion of First Class Load	0.12
	The Proportion of Third Class Load	0.12
	Daily Average Electricity Consumption	0.15
	Daily Average Peak and Valley Difference	0.25
	Natural Fluctuation Rate of Load	0.11
	The Percentage of Interruptible Load	0.25
Willingness of Load Interruption	The Percentage of Electric Bill	0.12
	The Adjusting Cost of Per Unit of Power	0.22
	Interruptible Capacity	0.26
	Interruptible Time	0.26
	The Speed of Response	0.14

TABLE 7. The evaluation results of adjustable potential of large industrial loads.

User Object	Score
Load 1	29.31
Load 2	59.99
Load 3	66.15
Load 4	57.36
Load 5	57.99
Load 6	48.55
Load 7	65.31
Load 8	64.69

TABLE 8. The division results of interrupt priority of large industrial loads.

User Object	Priority of Load Interruption	Coefficient of Adjusting Cost
Load 1	4	1.8
Load 2	1	1.2
Load 3	0	1.0
Load 4	2	1.4
Load 5	2	1.4
Load 6	3	1.6
Load 7	0	1.0
Load 8	0	1.0

TABLE 9. The assessment results of adjustable potential of large industrial load.

User Object	Score
Load 1	28.12
Load 2	50.12
Load 3	57.02
Load 4	49.06
Load 5	49.21
Load 6	45.19
Load 7	51.96
Load 8	52.69

generation side and load side in one day is studied. This paper takes the continuous three-stage rolling regulation (day-ahead, in-day and real-time) results in 24 hours as an example to analyze.

According to the linear weighted evaluation function method, the day-ahead optimization model and the in-day rolling adjustment model are transformed into single-target optimization models, as shown in Table 10 and Table 11.

TABLE 10. The selection result of compromise solution of the day-ahead optimization model.

Situation	f_{c1}	f_{p1}	Weight K_1	Weight K_2
Min(f_{c1})	3271287.33	48.66	0.56	0.44
Min(f_{p1})	4182195.47	21.45		

TABLE 11. The selection result of compromise solution of the in-day rolling model.

Situation	f_{c1}	f_{p1}	Weight K_1	Weight K_2
Min(f_{c1})	2876412.83	34.56	0.58	0.42
Min(f_{p1})	3985647.21	24.47		

Therefore, the objective function of the day-ahead model and the in-day model is transformed into the following function.

$$F_1' = 0.56 \times f_{c1} + 0.44 \times f_{p1} \tag{58}$$

$$F_2' = 0.58 \times f_{c2} + 0.42 \times f_{p2} \tag{59}$$

For demand-side resource regulation, it is necessary to minimize the cost of resource regulation while ensuring the effect of peak shaving and valley filling. The roles of the day-ahead and in-day model are mainly to arrange the electricity consumption plans of large industrial consumers belonging to the transferable and reducible loads. According to different types of load, a stack diagram representing the electricity load within one day is drawn, as shown in Figure 15.

In Figure 15, the gray part represents the important load which cannot be regulated, the red and blue parts represent the reducible and transferable load. It can be seen that the electricity users in this system have high regulation potential.

The specific optimal results of the day-ahead and in-day regulation for the flexible control of large industrial loads are shown in Table 12 and Table 13.

As can be seen from Table 12 and Table 13, on the basis of the interrupt priority, after the day-ahead and in-day

TABLE 12. The regulation results of the transferable load.

User Object	Variable that Controls Load Transfer	Time Period for Transferring Load	Time Period for Accepting Load
Load 1	0	—	—
Load 2	1	[26,45]	[77,96]
Load 3	1	[41,60]	[6,25]
Load 4	0	—	—

TABLE 13. The regulation results of the reducible load.

User Object	Variable that Controls Load Reduction	Time Period for Load Reduction	Capacity with Reduced Load
Load 5	0	—	—
Load 6	0	—	—
Load 7	1	[55,76]	14
Load 8	1	[25,48]	10

TABLE 14. The output arrangements of thermal power units.

Stage	Unit 1	Unit 2	Unit 3	Unit 4	Unit 5	Unit 6
In-day Output /MW	10649.3	9669.5	16609.7	12805.6	6052.1	556.80
Real-time Output /MW	10889.9	9305.5	16933.7	13160.2	5748.5	305.20

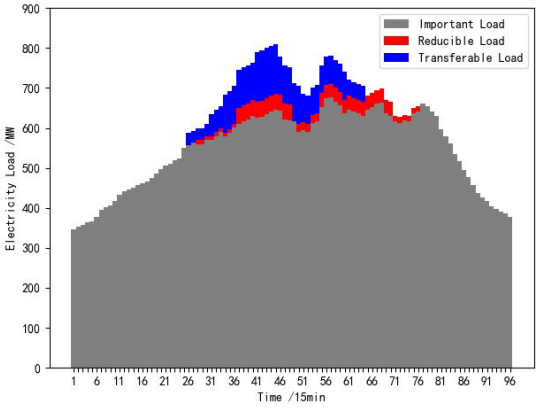

FIGURE 15. The diagram of different types of electricity load.

regulation, the electricity consumption plan of users with higher interruption priority (Load 2 and Load 3, Load 7 and Load 8) will be changed preferentially (transfer its electricity load in the peak period to the low period, or reduce the load in the peak period) to relieve the pressure of peak period and smooth load characteristic curve, in order to achieve the effect of 'peak-shaving and valley-filling'.

For the regulation of resources on the power generation side, it is necessary to pursue the economic optimization of the unit commitment on the basis of matching the demand-side power load to ensure sufficient power supply. The role of the day-ahead regulation is mainly to make the start-stop plan of thermal power units, and the role of the in-day regulation is mainly to determine the output of thermal power units on the basis of the start-stop plan. The specific optimization results of the day-ahead, in-day and real-time regulation for resources on the power generation side are shown in Table 14, in Figure 16 and in Figure 17.

Figure 16 shows the start-stop status of each thermal unit in 96 time periods in a day, where the red square represents the starting state, and the blue square represents the shutdown state. It can be seen that in order to ensure the maximum utilization of resources, the thermal power units with small capacity are basically in the start-up state during the trough period, but the thermal units with smaller capacity are shut down and the thermal units with larger capacity are started during the peak period.

Table 14 shows the total active power output of six thermal power units in the system through the in-day and real-time regulation. It can be seen that Unit 1∼4 undertakes most electric power supply, Unit 5 and Unit 6 mainly play a regulatory role, and the total output is relatively small. In addition, based on in-day regulation, real-time regulation is to immediately adjust and update the output arrangements of thermal power units according to the real-time changes of electrical load in the new day, in order to improve the reliability of the system.

It can be seen from Figure 17 that during the peak period [34], [80], the power supply is realized by Unit 1∼4, and the utilization efficiency of the units is maximized. Among them, Unit 1 and Unit 3 are basically in the state of full power generation. Unit 2 and Unit 4 appropriately increase and decrease the output, which plays the role of auxiliary regulation. By contrast, during the trough period, large units are shut down, and small units gradually start to avoid the waste of resources.

After fully determining the regulation scheme of power generation side and demand side, the cost of implementing regulation and the standard deviation after curve changes are calculated, as shown in Table 15. The load demand curve and the unit output curve before and after regulation are shown in Figure 18.

In Figure 18, the blue line represents the original load demand curve of the system, and the purple line and the red line represent the load demand curve and the units' output curve respectively after the three-stage rolling scheduling

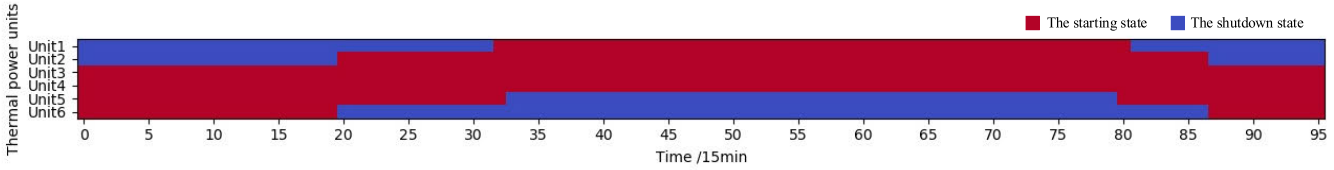

FIGURE 16. The color block diagram of start-stop plan of thermal power units.

TABLE 15. The economic dispatch results.

	Resource Regulation Cost (yuan)	Change in the Standard Deviation of the Load Curve
Start-stop Costs of Units	145478.6	
Operating Costs of Units	2815122.3	Before: 138.4
Costs of Load Transferring	317051.3	
Costs of Load Reduction	432564.7	After: 115.2
Summation	3710216.9	

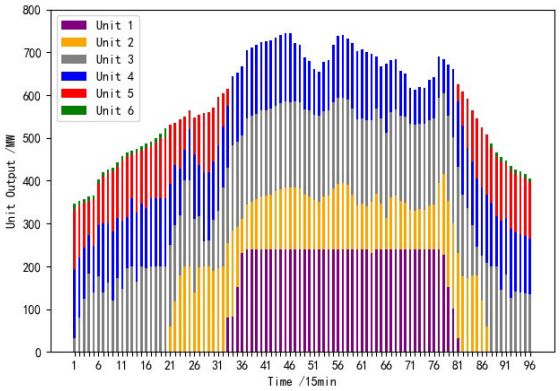

FIGURE 17. The bar chart of thermal power units' output.

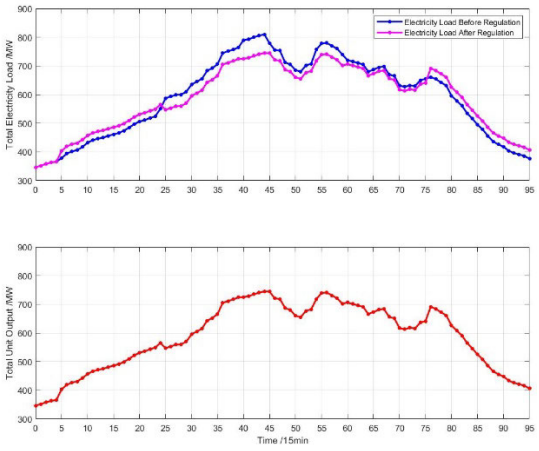

FIGURE 18. The effect diagram of three-stage rolling regulation.

of resources on the demand side. It can be seen that after regulation, the gentleness of the load characteristic curve is significantly improved, and electricity load during the peak period [25], [75] is significantly decreased, while the power load in the trough period is increased. The goal of 'peak-shaving and valley-filling' is well completed. At the same time, the total output curve of thermal power units is basically consistent with the load demand curve after regulation, which ensures the stable operation of the power system.

In addition, the economic dispatch results of this model are shown in Table 15.

From Table 15, it can be seen that on the basis of traditionally economic dispatch on the generation side, increasing the regulation of load side resources, the increased regulation cost accounts for about 20.2% of the total cost, and the standard deviation of the electricity load curve is also reduced by nearly 17%. Although the realization of load-side resource regulation increases some costs, the load peak-to-valley difference decreases, and the smoothness of the curve is significantly improved.

3) COMPARATIVE ANALYSIS OF DIFFERENT SCHEDULING MODELS

In view of the scheduling model established in this paper where the concepts of the IoT technology and the priority of load interruption are creatively introduced, the following will compare it with the model without IoT technology and the model without interrupt priority.

Model 1: The flexible regulation model of large industrial load based on IoT technology and interrupt priority proposed in this paper.

Model 2: The flexible regulation model of large industrial load, considering interrupt priority, without IoT technology.

Model 3: The flexible regulation model of large industrial load, based on IoT technology, without considering the priority of load interruption.

In Model 2, the Internet of Things technology is not applied, so Load 1 and Load 3, Load 5 and Load 7 can only be regarded as a whole object respectively, and cannot be controlled separately.

In Model 3, the concept of interruption priority is not used. The actual characteristics of large industrial consumers are not considered, and the flexible regulation scheme of large industrial loads is directly optimized.

TABLE 16. The results of transferable load regulation.

Model	User Object	Variable that Controls Load Transfer	Time Period for Transferring Load	Time Period for Accepting Load
Model 2	Load 1	1	[31,50]	[1,20]
	Load 2	1	[26,45]	[77,96]
	Load 3	1	[41,60]	[6,25]
	Load 4	0	—	—
Model 3	Load 1	1	[31,50]	[1,20]
	Load 2	1	[26,45]	[77,96]
	Load 3	0	—	—
	Load 4	0	—	—

TABLE 17. The results of reducible load regulation.

Model	User Object	Variable that Controls Load Reduction	Time Period for Load Reduction	Capacity with Reduced Load
Model 2	Load 5	1	[50,70]	20
	Load 6	0	—	—
	Load 7	1	[55,76]	14
	Load 8	1	[25,48]	10
Model 3	Load 5	1	[50,70]	20
	Load 6	1	[37,48]	30
	Load 7	1	[55,76]	14
	Load 8	0	—	—

TABLE 18. The comparison of economic dispatch results of different models.

	Model 1 (yuan)	Model 2 (yuan)	Model 3 (yuan)
Start-stop Costs of Units	145478.6	152987.4	135648.5
Operating Costs of Units	2815122.3	2796459.7	2695647.9
Costs of Load Transferring	317051.3	382065.9	342318.7
Costs of Load Reduction	432564.7	498026.3	514879.3
Summation	3710216.9	3829539.3	3688494.4

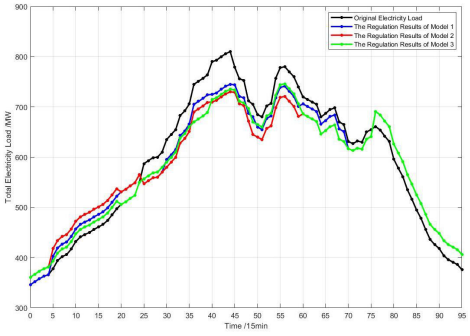

FIGURE 19. The comparison diagram of the effects of different scheduling models.

The regulation and optimization results of Model 2 and Model 3 for demand-side resources are shown in Table 16, Table 17 and Figure 19.

This article compares the effects of Model 1, Model 2 and Model 3 on demand-side resources regulation. For Model 2, it can be found that because the electricity load of a single large industrial consumer cannot be controlled in blocks, more load resources need to be regulated in order to meet certain requirements of peak regulation. For Model 3, due to ignoring the impact of load interruption priority, it may prioritize the adjustment of load objects with low adjustment potential, possibly causing some large industrial users who are not willing to stop using electricity to breach the contract, or have a greater impact on their production and operation activities.

As shown in Table 12, Table 13, Table 16 and Table 17, in Model 1, only Load 2, Load 3, Load 7 and Load 8 need to be adjusted to achieve the requirements of peak regulation. While in Model 2, the adjustment of Load 1 and Load 5 is increased, which wastes part of the demand-side resources. In addition, in Model 3, Load 1, Load 5, and Load 6 with lower interrupt priority are adjusted preferentially, instead of Load 3 and Load 8 with higher interrupt priority.

Figure 19 shows the characteristics of power load before and after the regulation of Model 1, Model 2 and Model 3. The black line represents the original load curve without regulation, and the blue, red and green lines respectively represent the changed electricity load curve after the regulation of Model 1, Model 2 and Model 3. It can be seen that the Model 2 cuts more electricity load during the peak period, and more electricity load transfers to the trough period, which certainly increases the cost of regulation. The peak-shaving effect of Model 3 is similar to that of Model 1, achieving the goal of 'peak shaving and valley filling'.

In addition to the comparison of peak regulation effects, the economic dispatch results of Model 1, Model 2 and Model 3 are shown in Table 18.

It can be seen from Table 18 that, compared with the scheduling results of Model 1, the total regulation cost in Model 2 has increased by about 3%, and the regulation

cost of load-side resources accounts for the vast majority of the increased cost. It can be seen that the use of the IoT technology to achieve flexible regulation of large industrial loads reduces certain costs, and improves the feasibility of demand-side resource regulation. In Model 3, because only economic benefits are considered and the impact of interrupt priority is ignored, the total control cost is slightly reduced (only about 0.5%, which can be ignored). However, this regulation mode lays down potential hazards for the flexible regulation of large industrial loads, which may affect the stable operation of the power system.

VII. CONCLUSION

This paper proposes a flexible control architecture for controllable large industrial load on the basis of IoT technology. Based on this, it evaluates the adjustable potential of large industrial load objects and divides the interrupt priority of various loads through the clustering method. Then, with the goals of 'peak shaving and valley filling' and minimizing the cost of resource regulation on the power generation side and demand side, we constructed a three-stage rolling control model, considering interrupt priority, of the large industrial controllable loads participating in deep peak shaving of the power gird. The research conclusions are summarized as follows:

1) The flexible control framework for controllable large industrial load based on IoT technology has been built to provide a basis for the flexible control of the loads.

2) A method for dividing the interrupt priority of large industrial loads is proposed. The improved TOPSIS evaluation method is used to establish the adjustable potential evaluation model of large industrial loads, and then the clustering algorithm is used to divide the interrupt priority, which realizes the arrangement of the adjustment order of the loads.

3) The rolling control strategy of controllable large industrial loads which participate in the deep peak shaving of the power grid is proposed. Considering the two-way regulation of resources on the power generation side and the demand side comprehensively, a three-stage (day-ahead, in-day and real-time) rolling control model has been established, which can effectively reduce peak-valley difference, smooth the load characteristic curve, and ensure the economy of system to a certain extent.

APPENDIX

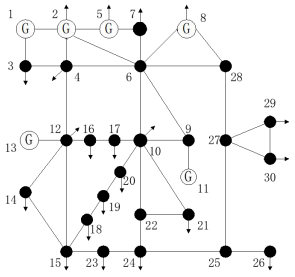

FIGURE 20. The improved IEEE 30-node system.

REFERENCES

[1] A. A. Hadi, C. A. S. Silva, E. Hossain, and R. Challoo, "Algorithm for demand response to maximize the penetration of renewable energy," *IEEE Access*, vol. 8, pp. 55279–55288, 2020.

[2] K. Mahmud, M. S. H. Nizami, J. Ravishankar, M. J. Hossain, and P. Siano, "Multiple home-to-home energy transactions for peak load shaving," *IEEE Trans. Ind. Appl.*, vol. 56, no. 2, pp. 1074–1085, Mar. 2020.

[3] H. Liang, Y. Liu, F. Li, and Y. Shen, "Dynamic economic/emission dispatch including PEVs for peak shaving and valley filling," *IEEE Trans. Ind. Electron.*, vol. 66, no. 4, pp. 2880–2890, Apr. 2019.

[4] J. Li, Y. Fu, Z. Xing, X. Zhang, Z. Zhang, and X. Fan, "Coordination scheduling model of multi-type flexible load for increasing wind power utilization," *IEEE Access*, vol. 7, pp. 105840–105850, 2019.

[5] M. F. Moghadam, M. Metcalfe, W. G. Dunford, and E. Vaahedi, "Demand side storage to increase hydroelectric generation efficiency," *IEEE Trans. Sustain. Energy*, vol. 6, no. 2, pp. 313–324, Apr. 2015.

[6] A. A. Almehizia, H. M. K. Al-Masri, and M. Ehsani, "Integration of renewable energy sources by load shifting and utilizing value storage," *IEEE Trans. Smart Grid*, vol. 10, no. 5, pp. 4974–4984, Sep. 2019.

[7] J. Liu and J. Li, "A bi-level energy-saving dispatch in smart grid considering interaction between generation and load," *IEEE Trans. Smart Grid*, vol. 6, no. 3, pp. 1443–1452, May 2015.

[8] M. Yu, S. H. Hong, Y. Ding, and X. Ye, "An incentive-based demand response (DR) model considering composited DR resources," *IEEE Trans. Ind. Electron.*, vol. 66, no. 2, pp. 1488–1498, Feb. 2019.

[9] P. Peng, Y. Li, D. Li, Y. Guan, P. Yang, Z. Hu, Z. Zhao, and D. Liu, "Optimized economic operation strategy for distributed energy storage with multi-profit mode," *IEEE Access*, vol. 9, pp. 8299–8311, 2021.

[10] A. Gholian, H. Mohsenian-Rad, and Y. Hua, "Optimal industrial load control in smart grid," *IEEE Trans. Smart Grid*, vol. 7, no. 5, pp. 2305–2316, Sep. 2016.

[11] K. Ma, G. Hu, and C. J. Spanos, "A cooperative demand response scheme using punishment mechanism and application to industrial refrigerated warehouses," *IEEE Trans. Ind. Informat.*, vol. 11, no. 6, pp. 1520–1531, Dec. 2015.

[12] M. Weyrich and C. Ebert, "Reference architectures for the Internet of Things," *IEEE Softw.*, vol. 33, no. 1, pp. 112–116, Jan. 2016.

[13] S. Uludag, K.-S. Lui, W. Ren, and K. Nahrstedt, "Secure and scalable data collection with time minimization in the smart grid," *IEEE Trans. Smart Grid*, vol. 7, no. 1, pp. 43–54, Jan. 2016.

[14] S. Din, A. Ahmad, A. Paul, M. M. U. Rathore, and J. Gwanggil, "A cluster-based data fusion technique to analyze big data in wireless multi-sensor system," *IEEE Access*, vol. 5, pp. 5069–5083, 2017.

[15] F.-C. Gu, S.-D. Lu, J.-X. Wu, C.-L. Kuo, C.-H. Lin, and S.-J. Chen, "Interruptible power estimation and auxiliary service allocation using contract theory and dynamic game for demand response in aggregator business model," *IEEE Access*, vol. 7, pp. 129975–129987, 2019.

[16] L. Yimin, Z. Jiahuan, Y. Xinping, N. Siqing, Z. Shaoming, and X. Ancheng, "A comprehensive evaluation method for relay protection based on expert investigation and G1 method," *Power Syst. Technol.*, vol. 44, no. 9, pp. 3533–3539, 2020.

[17] H. Shi, Y. Li, Z. Jiang, and J. Yan, "Comprehensive evaluation of power quality for microgrid based on CRITIC method," in *Proc. IEEE 9th Int. Power Electron. Motion Control Conf. (IPEMC-ECCE Asia)*, Nov. 2020, pp. 1667–1669.

[18] Z. Zhou, G. Wu, X. Dong, Y. Xue, C. Wang, and R. Shi, "An comprehensive assessment model for the distribution network with the new type of loads based on the TOPSIS method," in *Proc. 2nd IEEE Conf. Energy Internet Energy Syst. Integr. (EI2)*, Oct. 2018, pp. 1–5.

[19] K. P. Sinaga and M.-S. Yang, "Unsupervised K-means clustering algorithm," *IEEE Access*, vol. 8, pp. 80716–80727, 2020.

[20] C. Yang, Z. Huijuan, Z. Wuzhi, H. Xinxin, and Z. Yuting, "Day-ahead-day two-stage rolling optimal dispatch considering generalized energy storage and thermal power combined peak shaving," *Power Syst. Technol.*, vol. 45, no. 1, pp. 10–20, 2021.

[21] F. Lei, L. Xia, and X. Fuzhen, "Simulation of residual stress of steam turbine welded rotor and its influence on fatigue life," *Proc. Chin. Soc. Elect. Eng.*, vol. 34, no. 17, pp. 2851–2860, 2014.

[22] S. Wang, Y. Sha, J. Cao, Y. Yang, W. Cheng, and Y. Chen, "Research and application of gas emissions assessment system of thermal power units," in *Proc. 5th Int. Conf. Inf. Sci. Control Eng. (ICISCE)*, Jul. 2018, pp. 917–921.

[23] T. Kuo, Z. Ming, Y. Fan, X. Song, and D. Jun, "Dynamic economic dispatch model considering environmental protection cost and wind power connection impact," *Power Syst. Technol.*, vol. 35, no. 6, pp. 55–59, 2011.
[24] Y. Yang, K. Luan, and B. Yang, "Precise analysis of interruption response rate and interruptible capacity of large users," in *Proc. IEEE 3rd Conf. Energy Internet Energy Syst. Integr. (EI2)*, Nov. 2019, pp. 520–524.
[25] Y. Wei, Z. Yang, and H. Liu, "Optimal dispatching strategy of load aggregators considering peak load shifting," in *Proc. IEEE Innov. Smart Grid Technol.-Asia (ISGT Asia)*, May 2019, pp. 2661–2665.

GUANGYU CHEN was born in Nanjing, China, in 1980. He received the doctor's degree in power system and its automation from Hohai University, in 2016. He has served as a Lecturer for Nanjing Institute of Technology, in February 2017, where he was promoted to an Associate Professor, in July 2020. His research interests include power system operation and control, large power grid optimal dispatch, line loss analysis, integrated energy, and electric vehicles.

XIN ZHANG was born in Taizhou, China, in 1996. He received the B.E. degree from Nanjing Institute of Technology, Nanjing, Jiangsu, China, in 2019, where he is currently pursuing the M.S. degree in electrical engineering. His current research interests include dispatching operation of power grid and demand side management.

CHUNHU WANG was born, in January 1976. He received the degree in power system and automation and the M.Eng. degree in electrical engineering from Northeast Electric Power University, in July 1999 and December 2013, respectively. He is currently the Deputy Director of the Power Dispatching Control Center, Planning Department, State Grid Heilongjiang Electric Power Company Ltd., where he has obtained the title of a Senior Engineer. His research interest includes optimal operation of power systems.

YANGFEI ZHANG was born in Yancheng, China, in 1970. He received the Ph.D. degree in electric system and its automation from Hohai University, in 2009. In August 2013, he became a Professor at Nanjing Institute of Technology. His research interests include power system operation and control, and new energy generation and utilization.

SIPENG HAO was born in Yangzhou, China, in 1971. He received the Ph.D. degree in electric system and its automation from Southeast University, in January 2009. In July 2015, he became a Professor at Nanjing Institute of Technology. He is mainly involved in the research work of low frequency oscillation of power systems and wind electric field equivalent modeling.